Biophysical Chemistry, 46 (1993) 153–163
Elsevier Science Publishers B.V., Amsterdam

BIOCHE 01731

Thermodynamical model of mixed aggregation of intercalators with caffeine in aqueous solution

Jan Kapuscinski [a] and Marek Kimmel [b]

[a] *The Cancer Research Institute, New York Medical College, Elmsford, NY 10523 (USA)*
[b] *Department of Statistics, Rice University, Houston, TX 77251 (USA)*

(Received 23 April 1992; accepted in revised form 12 October 1992)

Abstract

Recently we presented evidence that some intercalating antitumor agents can form complexes with caffeine and that this process may be responsible for the modifying effect of caffeine on the pharmacological activity of these drugs (F. Traganos et al., Cancer Res. 51 (1991) 3682). Here we describe a statistical–thermodynamical model of mixed associations in which one component's self-association is limited to dimer formation while the second component has the ability of unlimited stacking. The system is controlled by three parameters which represent self-aggregation "neighborhood" association constants K_{CC} and K_{AA} and a mixed "neighborhood" association constant K_{AC}. The model was tested using acridine orange and light absorption spectroscopy as an analytical method for detection of complex formation. The experiments performed at two NaCl concentrations (0.01 and 0.15 M) indicate interesting properties of the three-parameter system in which the first parameter (K_{CC}) is practically independent of ionic strength, the second (K_{AA}) is positively and the third parameter (K_{AC}) is adversely affected by ionic strength.

Keywords: Caffeine; Acridine orange; Intercalator; Stacking interaction; Mixed association constant; Spectroscopy (light absorption)

1. Introduction

Caffeine (CAF, Fig. 1) has a multiplicity of effects on cells. It is a non-mutagenic compound [1], but at high concentrations (> 10 mM) prolongs the duration of G_1 phase [2,3], inhibits enzymes required for DNA synthesis [4,5], and causes increased chromatin condensation [6,7]. When combined with a wide variety of DNA-damaging agents (e.g., ionizing radiation, mitomycin C, cyclophosphamide and other alkylating

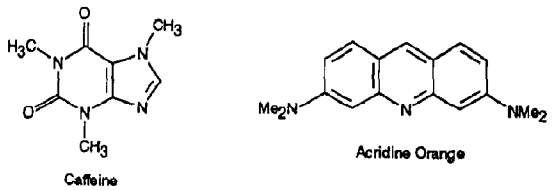

Fig. 1. Chemical structures of acridine orange (AO, 3,6-bis(dimethylamino)acridine hydrochloride) and caffeine (CAF, 3,7-dihydro-1,3,7-trimethyl-1 H-purine-2,6-dione).

Correspondence to: J. Kapuscinski, The Cancer Research Institute, New York Medical College, 100 Grasslands Rd., Elmsford, NY 10523.

agents, cisplatinum and its analogues, hydroxyurea, etc.), caffeine enhances cell killing, presumably by shortening the time of cell cycle arrest normally caused by such agents, thereby limiting the repair of potentially lethal DNA damage [8–13]. However, earlier reports [14–16] indicated that CAF can diminish the cytotoxic and/or cytostatic effects of doxorubicin. It also reduces the toxicity of ethidium bromide [17] and reverses the cytotoxic effects of antitumor agents mitoxantrone, ellipticine and the doxorubicin analogue AD198 [18]. These data raised the question, why does CAF potentiate toxic effects in one group of DNA damaging agents while having an opposite effect on the other group. The simplest explanation to this question would be a chemical interaction of some kind between CAF and the second group of drugs. Examination of the chemical structure of these compounds, however, indicates that formation of any covalently bound adduct between CAF and drugs in aqueous, neutral solutions and at room temperature is doubtful. In our recent paper [19] we presented evidence that CAF forms non-covalent (π–π or stacking) complexes with Mitoxantrone and the model intercalator acridine orange (AO, Fig. 1). The formation of CAF–drug complexes in solution effectively lowers the concentration of the free drug and thereby reduces its pharmacological activity.

The drugs in which pharmacological action was reduced by CAF are intercalators. When some intercalators are mixed with CAF, a multiple equilibria system is formed in which several types of interactions exist: (a) CAF, in solution, undergoes self-association to form indefinite-sized aggregates in equilibrium with a CAF monomer. There are several types of such interactions [20] and it has been shown ([21], and the references cited therein), that in the case of CAF, the process is of the isodesmic type, i.e., $K_{1,2} = K_{2,3} = \ldots = K_{n-1,n}$ [20]; (b) most intercalators also aggregate in aqueous solution; their aggregation in solutions in which their concentration is in the μM range is limited, however, to dimer formation [22—24]; (c) spectroscopic studies [19] indicate mixed CAF–drug aggregate formation which are in equilibrium with CAF and drug monomers and CAF and drug aggregates.

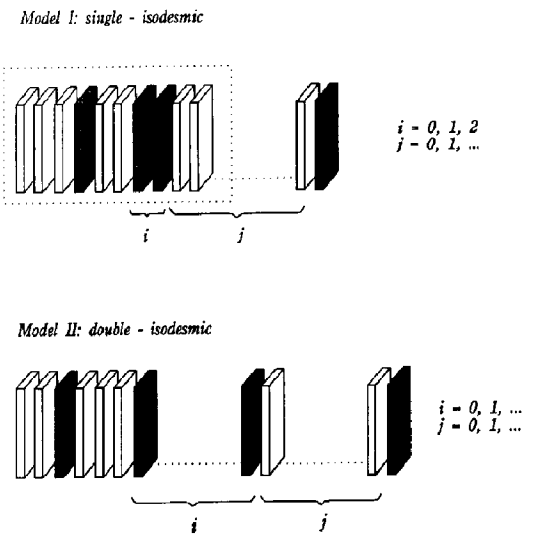

Fig. 2. Schematic representation of two models of mixed aggregation of AO (shadowed elements) and CAF. In both models, CAF forms aggregates of unlimited length (i.e., $j = 0, 1, 2, \ldots$), as does AO in the double isodesmic model (Model II). In the single isodesmic model (Model I), the length of AO aggregates is limited to two molecules (i.e., $i = 0, 1, 2$).

The aim of this study was to create a method for calculating free drug concentration in its mixture with CAF (based on the total component's concentrations) which would allow one, in turn, to correlate the effect of CAF on the pharmacological action of intercalating drugs.

It is known that CAF forms stacking complexes with nucleotides e.g., AMP ([21] and references cited therein) and an elegant statistical–thermodynamical model of indefinite mixed association of these components was developed by Weller et al. [25]. In this model, which we will call double-isodesmic, or Model II (Fig. 2), both components, the CAF and AMP, can form indefinite stacks. In our system, however, aggregation of the one component is limited to dimerization only. In the literature, we have found only one attempt to build such a model, by Dimicoli and Hélène [26]. These authors, however, have not been able to find any simple representation for it. In this paper, we present a statistical–thermodynamical model of such a system which will be called the mono-isodesmic or Model I (Fig. 2). While it is possible, based on derived equations, to calculate

the concentration of any component present in the mixture, the calculations are focused on the relationship between the monomer of the intercalator and CAF concentration. To test the model, AO was chosen, because of its well known spectral and self-aggregation characteristics [22,23,27].

2. Materials and methods

Caffeine (CAF, Fig. 1), purchased from Sigma (St. Louis, MO), was dried under P_2O_5 and used without further purification; its stock solution (at a concentration of approximately 0.1 M) was prepared by dissolving its weighted amount in an appropriate buffer at 37°C. Acridine orange (AO, 3,6-bis(dimethylamino)acridine hydrochloride, Fig. 1), chromatographically purified, was obtained from Polysciences (Warrington, PA). A stock solution of AO was prepared in distilled water (approximately 1 mM) and its concentration was assayed colorimetrically at the isosbestic point using a molar absorption coefficient of $E_{470} = 4.33 \times 10^4\ M^{-1}\ \mathrm{cm}^{-1}$ [27].

Colorimetric titrations were performed using an IBM 9410 UV-visible spectrophotometer interfaced to an HP 9826 computer. The 2-ml aliquot containing AO (5–35 μM) dissolved in 5 mM Hepes (pH 6.8), 0.01 or 0.15 M NaCl was placed in a quartz cuvette (1 cm light path) in the thermostatic holder (25.0 ± 0.1°C) of the spectrophotometer and titrated with CAF stock solution. The absorption spectra were then measured at 1 nm intervals and stored in digital form. The spectra were corrected for the absorption of the buffer and expressed in the form of molar absorption coefficient (E_λ, $M^{-1}\ \mathrm{cm}^{-1}$).

3. Models

The two systems discussed here contain two types of molecules, A (e.g., AO) and C (CAF), which can form different self- and mixed aggregates. Relative concentrations of the components are calculated using the partition function Z of the system, which is obtained by adding the statistical weights of all the states accessible to all types of oligomers. The statistical weight of an oligomer is a number proportional to the frequency of occurrence of this oligomer in the mixture of all possible oligomers.

The principal hypothesis making the present model (Model I) different from that of Weller et al. [25] (Model II) is that component A may form aggregates of the length of 1 or 2 only, while the length of component C aggregates is unrestricted (in Model II both are unrestricted, Fig. 2). In the description of the models, we follow the notation and definitions used by Weller et al. [25]. Thus, the statistical weight of any oligomer contains: (1) a factor c_A for each A; (2) a factor c_C for each C; (3) a factor K_{AA} for each AA neighborhood; (4) a factor K_{CC} for each CC neighborhood; (5) a factor K_{AC} for each AC neighborhood ($K_{AC} = K_{CA}$, [25]). The terms c_A and c_C denote the concentration of isolated (i.e., free) A and isolated C molecules in solution. K_{AA}, K_{CC} and K_{AC} denote the nearest neighbor equilibrium constants of association of A with A, C with C and A with C, respectively. The relation between K_{AA} and dimerisation constant $K_D = [\mathrm{dimer}]/[\mathrm{monomer}]^2$ is: $K_{AA} = 2K_D$ [20,21,26]. A sample calculation is given in Fig. 2. A segment inside the rectangular dotted box has a statistical weight equal to $c_A^3 c_C^7 K_{AA} K_{CC}^4 K_{AC}^4$.

The statistical weight of pure C aggregates of length i (i ($i = 1, 2, \ldots$) is equal to $K_{CC}^{i-1} c_C^i$. This aggregate with two A type borders of lengths 0, 1, or 2 each has the weight,

$$K_{CC}^{i-1}\left(1 + K_{AC}c_A + \tfrac{1}{2}K_{AC}K_{AA}c_A^2\right)^2,$$

and with additional $(i-1)$ type A insertions of length 0, 1 or 2

$$c_{C,i} = K_{CC}^{i-1}\left(1 + K_{AC}c_A + \tfrac{1}{2}K_{AC}K_{AA}c_A^2\right)^2 \times \left[1 + \frac{K_{AC}^2}{K_{CC}}c_A + \frac{K_{AC}^2}{2K_{CC}}K_{AA}c_A^2\right]^{i-1}. \quad (1)$$

The sum of all $c_{C,i}$ ($i = 1, 2, \ldots$) provides the total statistical weights of all possible aggregates with the exception of those composed of pure A. The weights of these (length 1 or 2) add up to:

$$y = c_A + \tfrac{1}{2}K_{AA}c_A^2. \quad (2)$$

Therefore, the partition function is equal to

$$Z = y + \sum_{i=1}^{\infty} c_{c,i}, \tag{3}$$

which yields, after calculating the sum of the infinite geometric progression,

$$Z = y + \frac{c_C(1 + K_{AC}y)^2}{1 - c_C(K_{CC} + K_{AC}^2 y)}. \tag{4}$$

The total concentrations of A (c_A^t) and C (c_C^t), are computed in the usual way as

$$c_A^t + \sum_{i=1}^{\infty} i(\text{coefficient of} c_A^i \text{ in } Z) \equiv c_A \frac{\partial Z}{\partial c_A}, \tag{5}$$

and

$$c_c^t = \sum_{i=1}^{\infty} i(\text{coefficient of } c_C^i \text{ in } Z) \equiv c_C \frac{\partial Z}{\partial c_C}, \tag{6}$$

respectively. Carrying out the necessary differentiations, we obtain

$$c_A^t = c_A(1 + K_{AA}c_A)\left[\frac{1 - c_C(K_{CC} - K_{AC})}{1 - c_C(K_{CC} + K_{AC}^2 y)}\right]^2, \tag{7}$$

and

$$c_C^t = c_C\left[\frac{1 + K_{AC}y}{1 - c_C(K_{CC} + K_{AC}^2 y)}\right]^2. \tag{8}$$

These two equations enable one to calculate the unknown concentration c_C and constant K_{AC}, with the data being K_{AA}, K_{CC}, c_A^t, and c_C^t. The solution has to be found numerically (for more detail see Section 4).

It should be noted that for $c_C = 0$ and/or $K_{AC} = 0$, eq. (7) is transformed to:

$$c_A^t = c_A + K_{AA}c_A^2 \tag{9}$$

which is the correct equation for the total A concentration in the absence of any AC interaction; the second part of eq. (9) represents the concentration of A in dimers. Similarly, for $c_A = 0$ and/or $K_{AC} = 0$, eq. (8) transforms into

$$c_C^t = \frac{c_C}{(1 - K_{CC}c_C)^2}, \tag{10}$$

which is the well known expression for isodesmic self-aggregation [20,21,26].

Using the partition function in a way similar to that used to obtain eq. (7) and (8), it is possible to find the concentrations of neighborhoods AA, CC, and AC:

$$c_{AA} = K_{AA}\frac{\partial Z}{\partial K_{AA}} \equiv K_{AA}\frac{\partial Z}{\partial y}\frac{\partial y}{\partial K_{AA}} \equiv \tfrac{1}{2}c_A^2\left[\frac{1 - c_C(K_{CC} - K_{AC})}{1 - c_C(K_{CC} + K_{AC}^2 y)}\right]^2, \tag{11}$$

$$c_{CC} = K_{CC}\frac{\partial Z}{\partial K_{CC}} \equiv K_{CC}\left[\frac{c_C(1 + K_{AC}y)}{1 - c_C(K_{CC} + K_{AC}^2 y)}\right]^2, \tag{12}$$

$$c_{AC} = K_{AC}\frac{\partial Z}{\partial K_{AC}} \equiv K_{AC} \times \frac{2c_C y(1 + K_{AC}y)[1 - c_C(K_{CC} - K_{AC})]}{[1 - c_C(K_{CC} + K_{AC}^2 y)]^2}, \tag{13}$$

where y is as defined in eq. (2).

It should be remembered that c_{AA}, c_{CC}, and c_{AC} are *not* concentrations of dimers AA, CC, and AC, respectively. They count all neighborhoods in all possible oligomers. For example, in the oligomer AACCCACCA, there are, one AA, three CC, and four AC neighborhoods.

Let us note that the sum of the count of all neighborhoods in any oligomer is equal to its length minus 1,

$$\#(AA) + \#(CC) + \#(AC) = \#(A) + \#(C) - 1. \tag{14}$$

Multiplying the above by the statistical weight of the oligomer and summing over all possible oligomers, after rearrangement one obtains,

$$c_{AA} + c_{CC} + c_{AC} - c_A^t - c_C^t + Z = 0. \tag{15}$$

This "balance of neighborhoods" provides a useful check for the calculations. Let us note also that, in general, no partial balances of neighbor-

hoods of type AA, CC, or AC seem to exist. However, if free component concentrations of the system (e.g., c_A and c_C) are known, it is possible to calculate the molar concentrations of components in the A dimers and molar concentrations of C in only C aggregates. Let us denote the molar concentrations of A and C by x_{AA} and x_{CC}, respectively. Oligomers of pure A and pure C are in equilibrium with free components in solution. Therefore,

$$x_{AA} = K_{AA} c_A^2, \tag{16}$$

and (from eqs. 19 and 20 in ref. [25]),

$$x_{CC} = \frac{K_{CC} c_C^2}{1 - K_{CC} c_C} \left[2 + \frac{K_{CC} c_C}{1 - K_{CC} c_C} \right]. \tag{17}$$

Now, the molecular concentration of A and C bound in mixed oligomers (x_A^b and x_C^b, respectively) can be calculated based on the mass conservation law:

$$x_A^b = c_A^t - c_A - x_{AA} \tag{18}$$

and

$$x_C^b = c_C^t - c_C - x_{CC}. \tag{19}$$

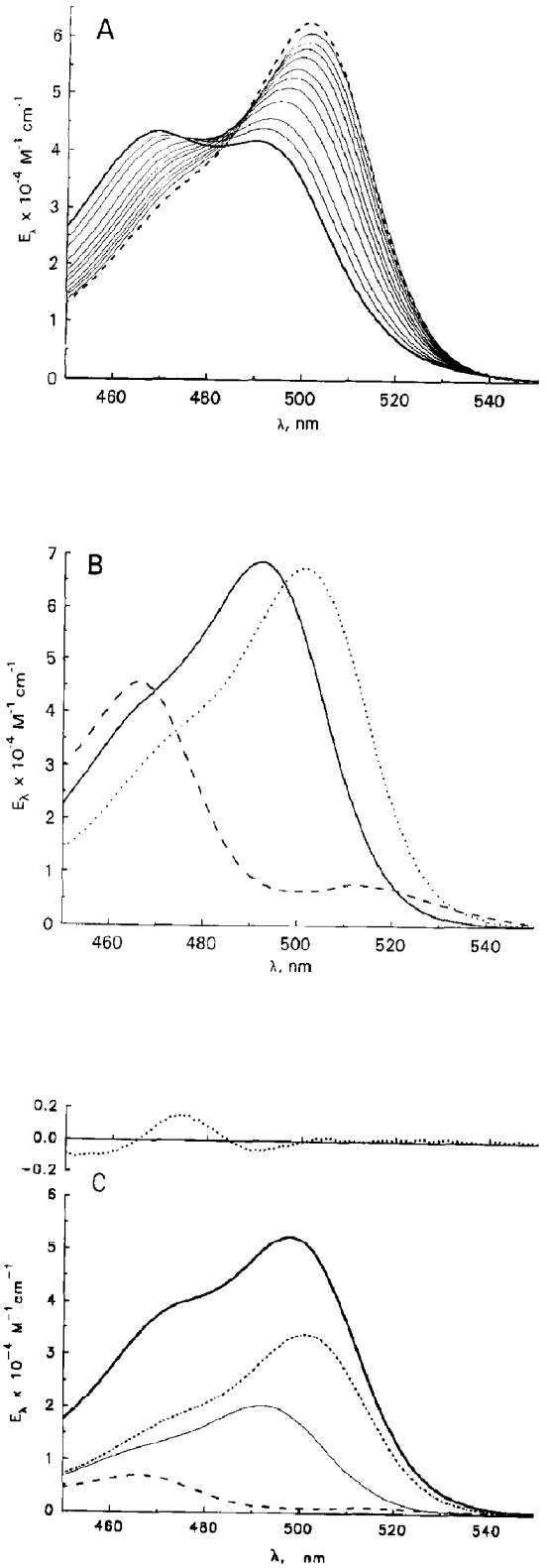

Fig. 3. Light absorption spectra measured in 0.15 *M* NaCl, 5 m*M* Hepes, pH 6.8. (A) titration of AO (initial concentration 32.4 μM) with CAF. (——) spectrum of AO alone; (—) AO/CAF ratio 0.067, 0.034, 0.017, 0.011, 0.0084, 0.0067, 0.0056, 0.0042, 0.0034, 0.0028 and 0.0022; (- - - - - -) extrapolated spectrum of AO monomer–CAF complex (AO/CAF → 0). (B) Comparison of the calculated spectra: (—) AO monomer and (- - - - - -) AO dimer (data from ref. [23]) and (· · ·) AO monomer–CAF complex (see A). (C) Three-parameter analysis (decomposition) of AO-CAF mixture (sample #5, Table 2). Under the spectrum of the mixture (——), there are spectra of the individual components listed in B, scaled in proportion to their molar fraction (θ_i) in the mixture: (—) AO monomer, (- - - - - -) AO dimer and (· · · · · ·) AO monomer–CAF complex. Top of (C): residue of the analysis (the difference between the measured and the weighted sum of the component spectra) indicates the presence of a fourth component in the mixture, as explained in the text.

4. Results and discussion

4.1 Analysis of the AO–CAF mixture

The absorption spectrum changes of AO titrated with CAF are presented in Fig. 3A. By extrapolation of $c_A^t/c_C^t \to 0$ the spectrum of the AO–CAF complex was calculated [19]. This spectrum represents the AO monomer associated with one or more CAF molecules. It should be pointed out that the changes in the spectra reflects the changes in electronic structure of AO only; CAF does not absorb above 350 nm. In previous studies in which NMR spectroscopy was used (e.g., [21,25]), it was possible to distinguish between inner ($\cdots$C–A–C$\cdots$) and outer A molecules (A–C$\cdots$) in aggregates since the former, having two neighbors, had twice the chemical shift as the latter. It seems that such discrimination is not possible in light absorption spectroscopy. Also, this technique is limited to chromophores which have an absorption band above 350 nm. This disadvantage, however, is overcome by the higher sensitivity of light absorption measurements, which allowed the study of interaction of some antitumor drugs with caffeine in micromolar (i.e., the pharmacological) concentrations [19].

The absence of an isosbestic point in the spectra presented in Fig. 3A indicate that more than two components are present in the mixture. The most obvious components of the mixture are the AO monomer, AO dimer and AO monomer associated with CAF. The spectra of these components are known [19] and are presented in Fig. 3B. It has been shown [19], that the spectrum of AO in the mixture with CAF, expressed as a molar absorption coefficient E_λ, can be decomposed into a weighted sum of components by nonlinear least squares regression analysis. The weighing parameter θ_i represents the molecular fraction of component i in the mixture ($\Sigma\theta_i = 1$). The best values for θ_i are those for which

$$\sum_\lambda \left[E_\lambda - \sum_{i=1}^{n} \theta_i E_{i,\lambda} \right]^2$$

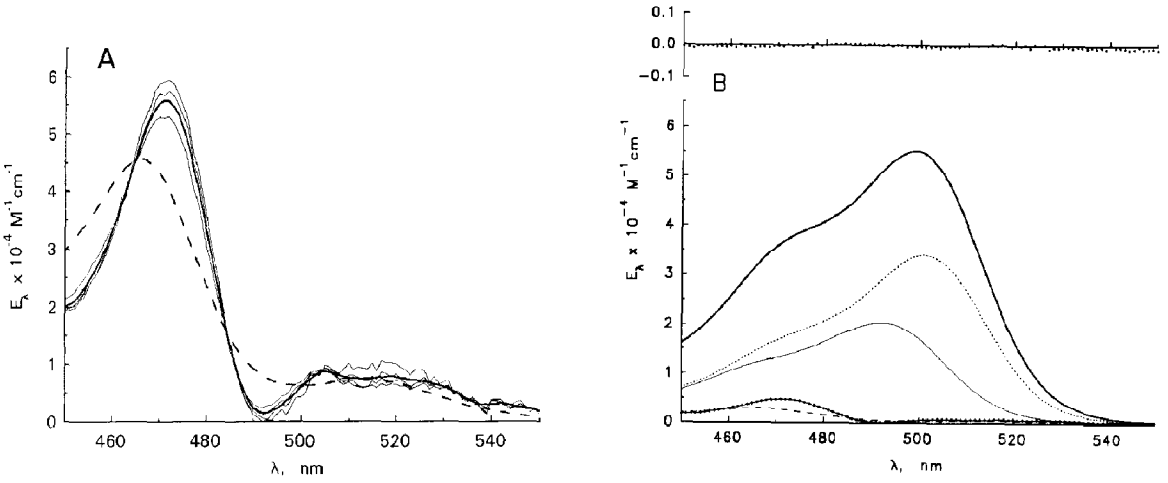

Fig. 4. (A) (—) spectra of the fourth component of the mixture contained AO, presumably AO dimer complexed with CAF. These spectra were calculated from spectra of samples #3–6 (Table 2) by subtracting the weighted component spectra of AO monomer, AO dimer and AO monomer–CAF complex, as described in the text; (——) The averaged and smoothed spectrum of the fourth component, which was used for four-parameter analysis. The maximum at 505 nm is an artifact resulting from noise in the buffer (blank) absorption measurement. Based on other experiments (not shown), it was established that the second, smaller maximum of the spectrum is at 520 nm. The spectrum of AO dimer (- - - - -) was added to the figure for comparison. (B) The four-parameter analysis of the sample described in Fig. 3(C). Under the spectrum of the mixture (——), there are spectra of the individual components, scaled in proportion to their molar fraction (θ_i) in the mixture: (—) AO monomer, (- - - - -) AO dimer, (· · · · ·) AO monomer–CAF complex and (–·–·–) AO dimer-CAF complex (see Fig. 4A). Top of (B): residue of the analysis.

is at minimum. $E_{i,\lambda}$ is the molar absorption coefficient component i at wavelength λ. For this calculation we used the Marquardt–Levenberg algorithm-based Sigmaplot program (Jandel Scientific, Corte Madera, CA).

In our previous paper [19], we use a three-component (i.e., AO monomer, AO dimer and AO monomer complexed with CAF) analysis of the mixture of AO and CAF. The concentration of AO in this earlier study, however, was small ($\sim 5\ \mu M$) and the ionic strength of the buffer was also low ($\sim 0.01\ M$). When we applied such treatment to the mixtures containing AO at a higher concentration ($\sim 30\ \mu M$) and at a NaCl concentration of 0.15 M, the results were less satisfactory (see Fig. 3C). In the lower part of the spectra, there were systematic fitting errors as indicated by the residues in Fig. 3C. Also, the measured concentration of the AO dimer was higher than expected (eq. 16), based on the measured AO monomer concentration. The latter parameter, as well as the concentration of AO monomer complex with CAF were measured correctly, as indicated by the calculation of these parameters over the 500–550 nm range (not shown). These symptoms indicated the presence of yet another component in the mixture, most likely AO dimer complexed with CAF. The spectrum of the fourth component of the mixture containing AO was obtained by subtraction from the spectrum of the mixture of those components related to AO monomer, AO monomer complexed with CAF and free AO dimer. The first two components were measured based on decomposition of the spectrum in the range of 500–550 nm; the concentration of the third component was calculated from eq. (16). The outcome of this procedure performed on spectra of four mixtures of AO and caffeine in different proportions is presented in Fig. 4A. The residue spectra obtained are similar to each other and this result strongly indicates the presence, in the mixture, of a fourth component containing AO. The spectrum of this component resembles the spectrum of the AO dimer but with a shift towards longer wavelengths (bathochromic shift), similar to that observed for the AO monomer complexed with CAF vs. AO monomer (Fig. 3B). The averaged spectrum of this component was then used for a four-parameter analysis of the AO–CAF mixtures (the spectral properties of identified complexes are summarized in Table 1). An example of this procedure is shown in Fig. 4B. and the results presented in Table 2. The standard error of spectra decomposition by this procedure was less than 0.001 in most cases and not higher than 0.005. These results were better than when the three-parameter analysis was used, as can be seen by comparison of the residues in Fig. 3C and Fig. 4B. The integrity of the four-parameter analysis was confirmed by decomposition of the spectrum of an AO solution (sample #0 in Table 2) which contained only AO monomer and dimer. The result of this decomposition was then used to calculate the AO dimerisation constant ($K_D = 2.12\ (\pm 0.01) \times 10^4\ M^{-1}$), which is in good agreement with previously published data, i.e. $K_D = 2.19\ (\pm 0.02) \times 10^4\ M^{-1}$ [23].

4.2 Calculation of the AO–CAF association constant K_{AC}

4.2.1 The single-isodesmic model (Model 1)

For calculation, we used the $K_{AA} = 11.3\ M^{-1}$ value reported by Fritzsche et al. [21], adjusted for 25°C, $K_{AA} = 2K_D = 4.24 \times 10^4\ M^{-1}$ as estimated above, and total concentrations of AO (c_A^t), CAF (c_C^t), and the measured free AO concentration (c_A, Table 2). K_{AC} was obtained by an iteration program using the relations described below.

Table 1

Spectral characteristics of AO and AO–CAF complexes in the 400–600 nm range at pH 6.8

	Absorption maxima λ, nm ($E_\lambda \times 10^{-4}\ M^{-1}\ cm^{-1}$)		Reference
AO monomer	492 (6.85)		[23]
AO dimer	466 (4.57)	515 (0.75)	[23]
AO monomer–CAF complex	501 (6.26)		This work
AO dimer–CAF complex	471 (5.61)	520 (0.78)	This work

Table 2

Titration of acridine orange with caffeine in 0.15 *M* NaCl, 5 m*M* Hepes, pH 6.8 at 25°C

Sample # (j)	Component total concentrations		AO molar fractions, θ_i				Component concentrations						
			Monomer	Dimer	Monomer complex	Dimer complex	c_A (μM) [c]	c_{AA} (μM)	c_C (mM)	c_{CC} (mM)	c_{AC} (μM)	x_{AA} (μM) [c]	x_A^b (μM) [c]
	c_A^t (μM)	c_C^t (mM)											
0	32.6	0	0.563	0.437	0.000 [b]	0.000 [b]	18.3	7.15	–	–	–	14.3	–
1	32.4	0.48	0.543	0.361	0.082	0.014	16.4	6.65	0.47	0.003	3.69	11.0	4.52
2	32.3	0.96	0.512	0.273	0.167	0.049	14.9	6.25	0.93	0.010	6.95	9.40	8.00
3	32.0	1.90	0.448	0.164	0.309	0.078	12.4	5.49	1.81	0.039	12.3	6.50	13.1
4	31.6	2.83	0.378	0.100	0.434	0.087	10.5	4.86	2.65	0.085	16.5	4.70	16.5
5	31.3	3.74	0.319	0.065	0.531	0.084	9.02	4.33	3.44	0.145	19.9	3.50	18.9
6	31.0	4.63	0.263	0.043	0.615	0.078	7.78	3.88	4.18	0.219	22.6	2.60	20.5
7	30.8	5.50	0.218	0.030	0.682	0.071	6.98	3.52	4.89	0.304	24.9	2.10	21.7
8	30.2	7.20	0.144	0.015	0.783	0.058	5.56	2.89	6.20	0.504	28.4	1.30	23.3

[a] Molar fractions were calculated from absorption spectra of the mixtures by four parameter analysis.

[b] Actual values were less then 10^{-7}.

[c] "Molecular" concentration of AO in monomer (c_A), dimer (x_{AA}), and AO–CAF complex (x_A^b).

Solving eq. (8) for c_C we obtain

$$c_C = \frac{2c_C^t B + A - \sqrt{A(4c_C^t B + A)}}{2c_C^t B^2}, \qquad (20)$$

where $A = (1 + K_{AC}y)^2$, $B = K_{CC} + K_{AC}^2 y$, and $y = c_A + \frac{1}{2}K_{AA}c_A^2$, from which a supposed total AO concentration $c_{AO,j}$ (subscript j designates here the titration point number listed in Table 2) using eq. (7) were calculated. The best value for K_{AC} is that for which

$$\sum_{j=1}^{m} \left(c_{AO,j} - c_{A,j}^t\right)^2$$

is minimal. Using $m = 8$ points of titration (Table 2), a $K_{AC} = 163\ (\pm 9)\ M^{-1}$ was established. Having this, all concentrations of neighbors can be calculated based on total component concentrations by a numerical method using eqs. (11)–(13). The results of these calculations are given in Table 2. The "molecular concentration" of AO monomer, dimer and AO–CAF complex were also calculated by this method and compared with data obtained by the four-parameter spectra analysis (Fig. 5A). There was good correlation between these data, with a standard error not exceeding 0.5 μM. The measurement of AO–CAF interaction in the buffer containing a low (0.01 M) NaCl concentration resulted in $K_{AC} = 258\ (\pm 7)\ M^{-1}$ (Table 3). It should be noted that K_{AC} is not very sensitive to K_{CC}. For instance, for the experimental condition described in Table 2, the change of its value from 6 to 24 M^{-1} resulted in a change in the K_{AC} value from 159 to 168 M^{-1}, respectively, i.e., less than a 6% increase.

Table 3

Parameters of the AO–CAF system (5 mM Hepes, pH 6.8 at 25°C) for both models

Associaton constants (M^{-1})	0.01 M NaCl		0.15 M NaCl	
	Model I	Model II	Model I	Model II
$K_{AA} \times 10^4$	2.91 [a]	1.34 [b]	4.25 [a]	1.37 [b]
K_{CC}	11.3	11.3	11.3	11.3
$K_{AC} \pm$ Se [c]	258 ± 7	247 ± 8	163 ± 9	99 ± 16

AO self-aggregation constant K_{AA} was obtained from the spectrum of an AO solution in the absence of CAF (e.g., sample #0, Table 2).

[a] Calculated using eq. (9).

[b] Calculated according to eq. (10).

[c] Standard error.

4.2.2. *The double-isodesmic model (Model II)*

The data from the experiment described in Table 2 were used to calculate the K_{AC} value

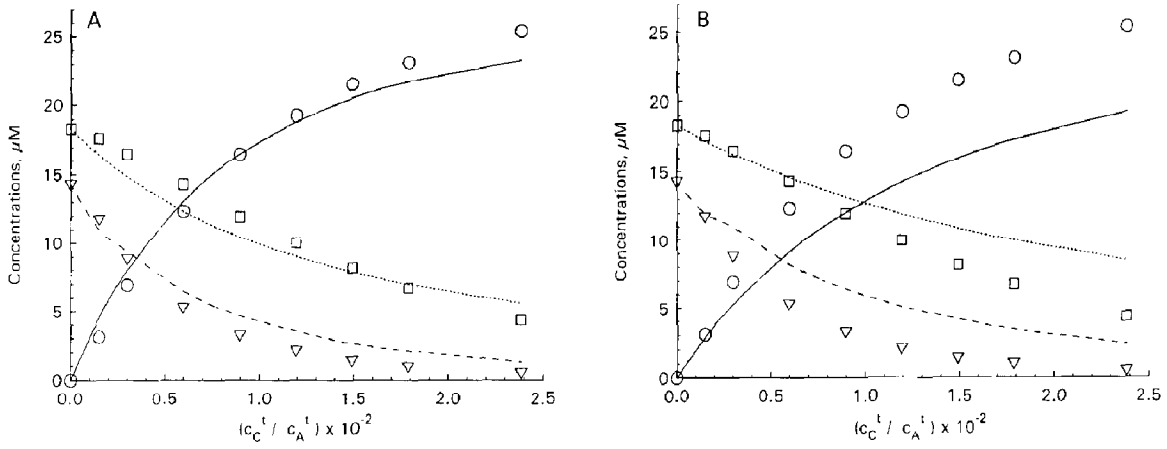

Fig. 5. The comparison of the results of four-parameter analysis of the mixtures of AO with CAF in 0.15 M NaCl, 5 mM Hepes pH 6.8, using data listed in Table 2 with values calculated using K_{AC} (Table 3) and total ligand concentrations (c_A^t and c_C^t, Table 2) for each point of titration (lines); (□ and ...) AO monomer (c_A), (▽ and - - - - - -) AO dimer (x_{AA}) and (○ and —) AO–CAF complex (x_A^b). (A) Calculations according to Model I; (B) according to Model II.

according to the model described by Weller et al. [25]. Resolving eq. (9) in ref. [25] for c_C we obtained

$$c_C = \left[1 - c_A K_{AA} - C\right]\left[c_A K_{AC}^2 + K_{CC}(1 - c_A K_{AA}) + C(K_{AC} - K_{CC})\right]^{-1}, \quad (21)$$

where $C = \sqrt{c_A / c_A^t}$. Then, K_{AC} was calculated by iteration, as described above for Model I, but using eqs. (16) and (18) in ref. [25]. For this model, however, K_{AA} was recalculated into the isodesmic association constant according to eq. (10). The result of the comparison between measured and calculated AO concentrations is presented in Fig. 5B. The numerical values of parameters for Model II are presented in Table 3. The results of experiments in a solution of low ionic strength are also included in Table 3.

It seems that at higher ionic strength and AO concentration, the single-isodesmic model (Model I) is much better than Model II in describing AO–CAF interactions (see Fig 5). In lower ionic strength buffer and at low AO concentrations, however, both models fit the experimental data well (not shown). The numerical values for K_{AA} used in the calculation were different for the two Models and resulted in different values for K_{AC} (Table 3).

4.3 Effect of ionic strength on the system

The equilibrium in the AO–CAF system is controlled by three parameters, i.e., K_{AA}, K_{CC} and K_{AC} which represent AO–AO, CAF–CAF and AO–CAF interactions, respectively. A short-range stacking interaction including hydrophobic and dispersive forces are the driving force for these associations. These forces are not supposed to be affected by changes in ionic strength. At a pH close to 7, however, AO is completely protonated ($pK_a = 10.4$ at 20°C) [28] and this introduces a long-range electrostatic interaction to the system [22]. At low concentrations (up to 50 μM), the repulsive electrostatic forces reduce self-aggregation of AO to dimer formation only [22], and the process is strongly affected by electrolytes. According to Robinson et al. [22], for AO, the log K_D (dimerisation constant) is proportional to the square root of ionic strength, as predicted by the Debye–Hückel theory. The increase of NaCl concentration from 0.01 to 0.15 M resulted in an increase of K_D from 1.46×10^4 to 2.12×10^4 M^{-1}. On the other hand, CAF is not charged at neutral pH and, therefore, K_{CC} is not expected to be sensitive to changes in ionic strength. A microcalorimetric titration indicates that, indeed, an increase in NaCl concentration from 0 to 0.15 M resulted in only a 7% increase in the K_{CC} value (unpublished data). The increase in K_{AC} with a decrease of ionic strength indicates that, perhaps, there is an ionic component in stacking interactions between AO and CAF and that, in the complex, the CAF molecule has some negative charge; if the CAF molecule was positively charged, the opposite relationship between K_{AC} and ionic strength would be expected. The AO–CAF system represents, therefore, an interesting case of a multi-equilibria system in which, among three control parameters, one (K_{CC}) is practically independent of ionic strength, while the second (K_{AA}) is positively and the third (K_{AC}) adversely affected by ionic strength.

Acknowledgements

We are greatful to Drs. Zbigniew Darzynkiewicz and Frank Traganos for their helpful discussion and Ms Irene L. Longsdon for her assistance in the preparation of the manuscript. This work was supported in part by NIH R37 CA23296 and NSF DMS 7903023 grants.

References

1 R.R. Ariza, G. Dorado, M. Barbancho and C. Pueyo, Mutat. Res. 201 (1988) 89.
2 F.J. O'Nail, J. Cell Physiol. 101 (1979) 201.
3 G. Iliakis and M. Nusse, Int. J. Radiat. Biol. 43 (1983) 649.
4 K.L. Beetham, P.M. Busse and L.J. Tolmach, J. Cell Physiol. 115 (1983) 283.
5 C.P. Selby and A. Sancae, Proc. Natl. Acad. Sci. U.S.A. 87 (1990) 3522.
6 V.M. Borodina, E.E. Kirianova, O.V. Federova and A.V. Zelenin, Exp. Cell Res. 122 (1979) 391.

7 J.E. Kunicka, A. Myc. M.R. Melamed and Z. Darzynkiewicz, Cell Tissue Kinet. 23 (1990) 31.
8 Roberts J.J., in: Caffeine, ed. P.B. Dews (Springer-Verlag, Berlin, 1984) p. 239.
9 V.J. McKelvey and P.G. McKenna, Mutagenesis 1 (1986) 173.
10 D. Mourelatos, J. Dozi Vassiliades, A. Kotsis and C. Gourtsas, Cancer Res. 48 (1988) 1129.
11 J.J. Roberts and V.P. Kotsaki Kovatsi, Mutat. Res. 165 (1986) 207.
12 H.C. Andersson and B.A. Kihlman, Mutat. Res. 181 (1987) 173.
13 D.A. Dawson and J.A. Bantle, Teratology. 35 (1987) 221.
14 W.E. Ross, L.A. Zwelling and K.W. Kohn, Int. J. Radiat. Oncol. Biol. Phys. 5 (1979) 1221.
15 R. Ganapathi, D. Grabowski, H. Schmidt, A. Yen and G. Iliakis, Cancer Res. 46 (1986) 5553.
16 G. Iliakis, M. Nusse, R. Ganapathi, J. Egner and A. Yen, Int. J. Radiat. Oncol. Biol. Phys. 12 (1986) 1987.
17 H. Kimura and T. Aoyama, J. Pharmacobiodyn. 12 (1989) 589.
18 F. Traganos, B. Kaminska Eddy and Z. Darzynkiewicz, Cell Prolif. 24 (1991) 305.
19 F. Traganos, J. Kapuscinski and Z. Darzynkiewicz, Cancer Res. 51 (1991) 3682.
20 L-H. Tang, D.R. Powell, B.M. Escott and E.T. Adams Jr., Biophys. Chem. 7 (1977) 121.
21 H. Fritzsche, I. Petri, H. Schütz, K. Weller, P. Sedmera and H. Lang, Biophys. Chem. 11 (1980) 109.
22 B.H. Robinson, A. Löffler and G. Schwarz, J. Chem. Soc., Faraday Trans. 1 69 (1973) 56.
23 J. Kapuscinski and Z. Darzynkiewicz, J. Biomol. Struct. Dyn. 5 (1987) 127.
24 J. Kapuscinski and Z. Darzynkiewicz, Biochem. Pharmacol. 34 (1985) 4203.
25 K. Weller, H. Schutz and I. Petri, Biophys. Chem. 19 (1984) 289.
26 J.-L. Dimicoli and C. Hélène, J. Am. Chem. Soc. 95 (1973) 1036.
27 V. von Tscharner and G. Schwarz, Biophys. Struct. Mechanism 5 (1979) 75.
28 V. Zanker, Z. Phys. Chem. 199 (1952) 225.